ACS chemical biology

pubs.acs.org/acschemicalbiology

Letters

High-Throughput Activity Assay for Screening Inhibitors of the SARS-CoV-2 Mac1 Macrodomain

Morgan Dasovich,[+] Junlin Zhuo,[+] Jack A. Goodman,[+] Ajit Thomas,[+] Robert Lyle McPherson, Aravinth Kumar Jayabalan, Veronica F. Busa, Shang-Jung Cheng, Brennan A. Murphy, Karli R. Redinger, Yousef M. O. Alhammad, Anthony R. Fehr, Takashi Tsukamoto, Barbara S. Slusher, Jürgen Bosch,* Huijun Wei,* and Anthony K. L. Leung*

Cite This: https://doi.org/10.1021/acschembio.1c00721

ABSTRACT: Macrodomains are a class of conserved ADP-ribosylhydrolases expressed by viruses of pandemic concern, including coronaviruses and alphaviruses. Viral macrodomains are critical for replication and virus-induced pathogenesis; therefore, these enzymes are a promising target for antiviral therapy. However, no potent or selective viral macrodomain inhibitors currently exist, in part due to the lack of a high-throughput assay for this class of enzymes. Here we developed a high-throughput ADP-ribosylhydrolase assay using the SARS-CoV-2 macrodomain Mac1. We performed a pilot screen that identified dasatinib and dihydralazine as ADP-ribosylhydrolase inhibitors. Importantly, dasatinib inhibits SARS-CoV-2 and MERS-CoV Mac1 but not the closest human homologue, MacroD2. Our study demonstrates the feasibility of identifying selective inhibitors based on ADP-ribosylhydrolase activity, paving the way for the screening of large compound libraries to identify improved macrodomain inhibitors and to explore their potential as antiviral therapies for SARS-CoV-2 and future viral threats.

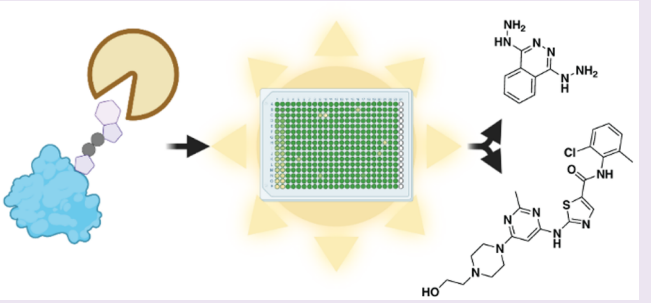

Seven human coronaviruses have been identified: HCoV-229E, HCoV-NL63, HCoV-OC43, and HCoV-HKU1 are responsible for annual bouts of the common cold, whereas SARS-CoV, SARS-CoV-2, and MERS-CoV can cause severe pneumonia and are a major public health concern. Hundreds of additional coronaviruses are circulating in animal reservoirs and could be transmitted to humans.[1] The diseases that result from zoonotic transfer are unpredictable but historically are severe and highly contagious and have potentially devastating consequences for public health. Therefore, developing broad-spectrum therapeutics against coronaviruses is of timely importance and will prepare us for future epidemics.

The SARS-CoV-2 genome encodes 4 structural proteins, 9 accessory proteins, and 16 nonstructural proteins that are responsible for virus replication. COVID-19 antiviral development has focused on repurposing existing drugs to inhibit the enzymatic activities of proteins involved in SARS-CoV-2 replication, including viral RNA polymerases and proteases.[2] As was the case for HIV and Hepatitis C virus, an effective treatment for SARS-CoV-2 will likely require a combination of drugs to pre-empt possible drug resistance. Therefore, identifying mechanistically distinct targets will complement current drug development efforts. Here we focus on screening for inhibitors of Mac1, a conserved macrodomain ADP-ribosylhydrolase within nonstructural protein 3 (nsp3).

The macrodomain is a protein fold found in humans and pathogens.[3−5] Nearly all of them bind to adenosine diphosphate ribose (ADP-ribose).[4−7] Recent data revealed that a subset of macrodomains hydrolyzes protein-conjugated ADP-ribose.[8−13] For example, SARS-CoV, SARS-CoV-2, and MERS-CoV contain two to three macrodomains in tandem, where only the first one (called Mac1) possesses ADP-ribosylhydrolase activity.[13−17] Notably, key residues critical for ADP-ribosylhydrolase activity are 100% conserved in all seven human coronaviruses as well as those identified from animal reservoirs, such as the bat (Figure S1). Macrodomain ADP-ribosylhydrolases are also conserved in another genus of pathogenic RNA viruses called alphaviruses (e.g., Chikungunya virus).[11,12] Genetic evidence demonstrates the ADP-ribosylhydrolase activity of viral macrodomains is critical for replication and virulence.[11,13,18−21] Mutant coronaviruses and alphaviruses cannot replicate when the ADP-ribose-binding sites within

Received: September 14, 2021
Accepted: November 16, 2021

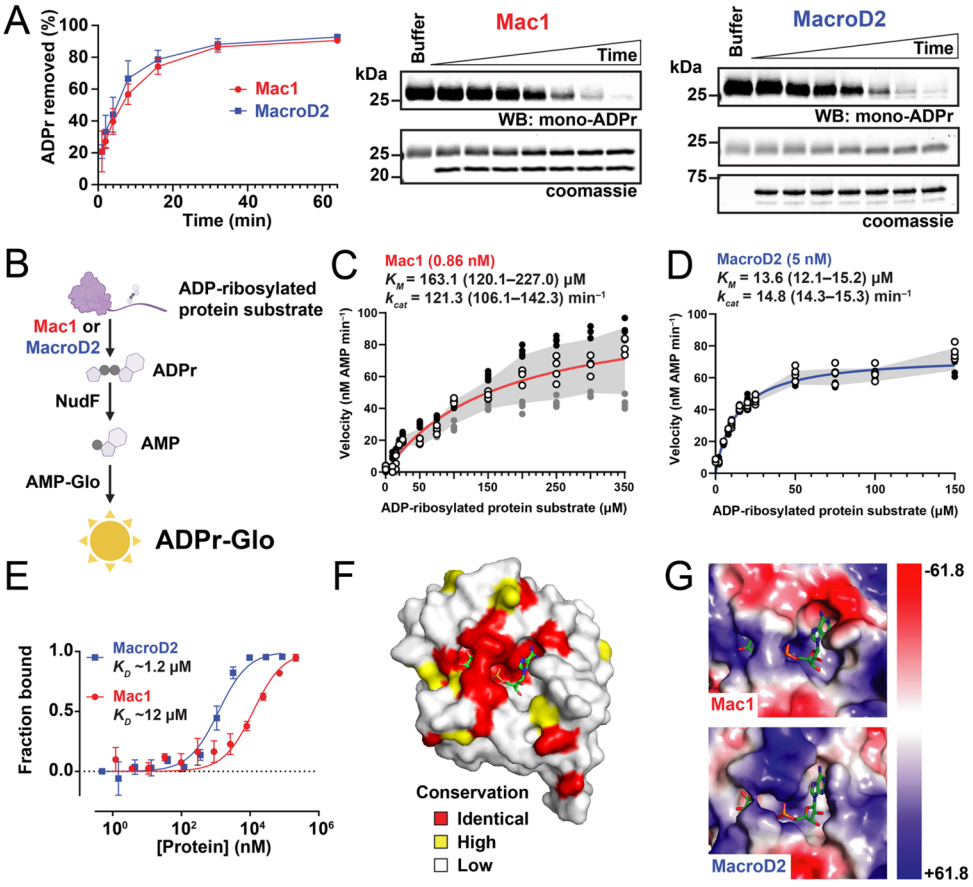

Figure 1. Biochemical, enzymatic, and structural characterization of SARS-CoV-2 Mac1 and human MacroD2. (A) Gel-based ADP-ribosylhydrolase assay against a mono-ADP-ribosylated substrate. Mono-ADP-ribose signal was normalized to the buffer signal. Plotted values are mean ± SD (n = 3). (B) Schematic of the luminescence-based ADP-ribosylhydrolase assay, ADPr-Glo. (C,D) Michaelis–Menten kinetics characterization of (C) Mac1 and (D) MacroD2 (n = 12, four technical replicates from three experiments; gray area is the SD). Kinetic parameters are best-fit values with the 95% confidence interval reported in parentheses. (E) Electrophoretic mobility shift assay (EMSA) analyses of Mac1 and MacroD2 with Cy5-PAR. Plotted values are the mean ± SD (n = 3). (F) Surface representation of the conservation between Mac1 and MacroD2. Bound ADP-ribose is shown as a stick representation, areas in red are identical, and areas in yellow are conserved. (G) Zoom-in view of the electrostatic surface potential of the ADP-ribose binding site for Mac1 (top) and MacroD2 (bottom).

their macrodomains are disrupted.[11,21] Additionally, macrodomain mutant viruses exhibit attenuated replication in differentiated cells and decreased virulence *in vivo*.[4,5] Therefore, drugs targeting the ADP-ribosylhydrolase activity of viral macrodomains have the potential to inhibit viral replication and pathogenesis.

Two major challenges must be addressed during the development of antiviral macrodomain inhibitors. First, measurements of macrodomain ADP-ribosylhydrolase activity have historically relied on gel-based autoradiography and Western blot assays that are not practical for screening large numbers of compounds. Second, humans express 11 proteins with macrodomain folds, such as MacroD2, which is the closest enzymatically active human homologue of SARS-CoV-2 Mac1.[15] Therefore, compounds that nonspecifically inhibit human macrodomains will likely have off-target effects that limit their utility. Here we describe a quantitative, high-throughput assay that identifies virus-specific and general inhibitors of macrodomains.

RESULTS AND DISCUSSION

To explore whether the selective inhibition of a viral macrodomain is possible, we began our investigation by identifying biochemical and structural differences between SARS-CoV-2 Mac1 and human MacroD2. Sequence analyses classified both Mac1 and MacroD2 macrodomains to the macroD-type subclass, which also includes the macrodomain from the Chikungunya virus.[3,5] Given that the Chikungunya virus macrodomain hydrolyzes ADP-ribose from the recombinant PARP10 catalytic domain[11,12] and G3BP1 protein from cells,[22] we tested these substrates with Mac1 and MacroD2 (Figure 1A and Figure S2A). Following macrodomain incubation, comparable losses of ADP-ribose signal from PARP10^{CD} and G3BP1 were observed, indicating that both SARS-CoV-2 Mac1 and human MacroD2 are active ADP-ribosylhydrolases.

To quantitatively measure the enzymatic activity with a high-throughput method, we developed the luminescence-based assay ADPr-Glo (Figure 1B): First, ADP-ribose is released from a defined protein substrate by the macrodomain ADP-ribosylhydrolase. Second, the phosphodiesterase NudF cleaves the released ADP-ribose into phosphoribose and AMP. Finally, AMP is converted to luminescence with the commercially available AMP-Glo kit. This method takes advantage of the substrate selectivity of NudF, which cleaves free ADP-ribose but has no activity with protein-conjugated ADP-ribose.[23] Therefore, the luminescence signal is controlled by the rate of the ADP-ribosylhydrolase. ADPr-Glo can be performed in 384-

https://doi.org/10.1021/acschembio.1c00721
ACS Chem. Biol. XXXX, XXX, XXX–XXX

well plates with reaction volumes as low as 5 μL, greatly minimizing time and costs compared with gel-based activity assays.

We first used ADPr-Glo to measure the Michaelis−Menten kinetics of SARS-CoV-2 Mac1 and human MacroD2 with an ADP-ribosylated protein substrate. The K_M of Mac1 was 163.1 μM with a k_{cat} of 121.3 min^{-1} (Figure 1C), and the K_M of MacroD2 was 13.6 μM with a k_{cat} of 14.8 min^{-1} (Figure 1D). The lower K_M of MacroD2 is consistent with its higher affinity for ADP-ribose monomers[16] and polymers (Figure 1E and Figure S2B). Therefore, SARS-CoV-2 Mac1 and human MacroD2 exhibit distinct binding and kinetic properties with free and protein-conjugated ADP-ribose, which likely reflect chemical and structural differences within their active sites.

A comparison of the published macrodomain structures of Mac1 and MacroD2 revealed that ∼60% of residues at the ADP-ribose binding sites are conserved (Figure 1F). An examination of the larger macrodomain family using 150 closely related sequences with 35−95% sequence identity showed cross-family conservation, in particular, for the ADP-ribose binding site (Figure S2C). Similar to MacroD2 and the Chikungunya virus macrodomain,[9,11] the mutation of a conserved glycine residue to glutamate (G252E for SARS-CoV-2 nsp3, Figure S1) abrogates the activity of Mac1 (Figure S2D). The incubation of Mac1 G252E with the ADP-ribosylated protein substrate followed by NudF addition yielded the same amount of signal as the NudF-only control. A closer examination of Mac1 and MacroD2 structures revealed less conserved regions (e.g., near the adenosine binding pocket; Figure 1F) and distinctive electrostatic surfaces surrounding the active site where ADP-ribose binds (Figure 1G and Figure S2E). Compared with MacroD2, Mac1 possesses a binding pocket with more charged surfaces that is 450 Å^3 larger (Figure 1G and Figure S2E,F). Taken together, these functional and structural differences may permit the selective inhibition of SARS-CoV-2 Mac1 but not human MacroD2.

We next established ADPr-Glo conditions for inhibitor screening (Figure 2A). The reaction was linear with respect to the enzyme concentration (0.5 nM) and the time of incubation (60 min) at room temperature in the presence of 20 μM ADP-ribosylated substrates, 125 nM NudF, and a final DMSO concentration of 1%, with excellent reproducibility when performed over different dates (Figure S3). We then carried out a pilot screen of the 3233 pharmacologically active compounds derived from the Selleck-FDA library (1953) and the LOPAC library (1280).

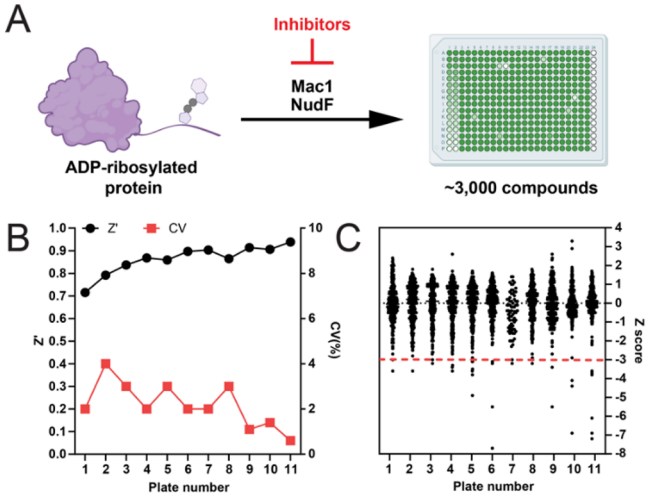

Figure 2. Pilot screen for macrodomain inhibitors. (A) Schematic of the drug screen based on the ADP-ribosylhydrolase assay ADPr-Glo. (B) Coefficients of variation (CV) and Z' values for each plate in the screen. (C) Z scores for the 3233 compounds evaluated.

The pilot screen parameters were suitable for a large high-throughput screen with the coefficient of variation (CV) ranging from 1 to 4%, the screening window coefficient Z' at 0.86, and an average signal-to-background (S/B) ratio of 3.4 (Figure 2B). We calculated the average signal (A) and standard deviation (SD) of compound-treated wells in each plate and determined a Z score for each compound where Z = (signal − A)/SD (Figure 2C). Compounds with Z score ≤ −3 were considered hits (Supplementary Data File 1).

Our pilot screen at 100 μM identified 21 compounds from the Selleck-FDA library and 16 compounds from the LOPAC library with Z ≤ −3, resulting in a 1.2% hit rate. Notably, the kinase inhibitor dasatinib was present as three different forms in the FDA library (Supplementary Data File 1), and all of them were identified as hits, indicating assay reproducibility. Among 37 total hits, 24 were excluded based on several criteria, including the presence of pan-assay interfering (PAINS) substructures or potential aggregators based on the ZINC filtering algorithm,[24] interference with luminescence detection, high molecular weight, instrument issues, or commercial availability. (See Supplementary Data File 1.) The remaining 13 hits were either purchased in powder form or synthesized for further evaluation.

To identify false-positive hits that either inhibit NudF or interfere with AMP detection by AMP-Glo, we performed a counter screen where 2 μM ADP-ribose was used instead of the ADP-ribosylated substrate and the macrodomain was omitted from the reaction (Figure S4A−F). Four compounds demonstrated dose-dependent inhibition in the counter screen, indicating that they are inhibitors of NudF or AMP-Glo (Figure S4B−E). Vandetanib had poor solubility in aqueous solution (<10 μM), which prohibited a dose−response analysis. The remaining six compounds did not inhibit the NudF-mediated counter-screen assay and were subsequently evaluated in a dose−response assay against SARS-CoV-2 Mac1 (Figure S4F−I).

Among the six remaining hits, only dasatinib and dihydralazine exhibited dose-dependent inhibition (Figure 3A,B and Figure S4G−I), with an IC_{50} of 37.5−57.5 μM and 486−757 μM (95% C.I.), respectively. We then evaluated these two inhibitors in an orthogonal gel-based activity assay. Consistent with its higher potency, only dasatinib mitigated the reduction of ADP-ribosylation under the tested conditions (Figure 3C).

To evaluate whether these drugs broadly inhibit ADP-ribosylhydrolases or are specific for Mac1, we replaced the SARS-CoV-2 macrodomain with human MacroD2 in our ADPr-Glo assay and tested for dose-dependent inhibition (Figure 3A,B). Strikingly, dasatinib did not show any inhibition of MacroD2, even at 2 mM, the solubility limit of the compound in 2% DMSO. On the contrary, dihydralazine inhibited MacroD2 and Mac1 with comparable potency (IC_{50} = 500−1830 μM, P = 0.82, t test).

Because dasatinib was more potent and selective, we focused our efforts on investigating the dasatinib−macrodomain interaction. To directly assess dasatinib binding to these two

https://doi.org/10.1021/acschembio.1c00721
ACS Chem. Biol. XXXX, XXX, XXX−XXX

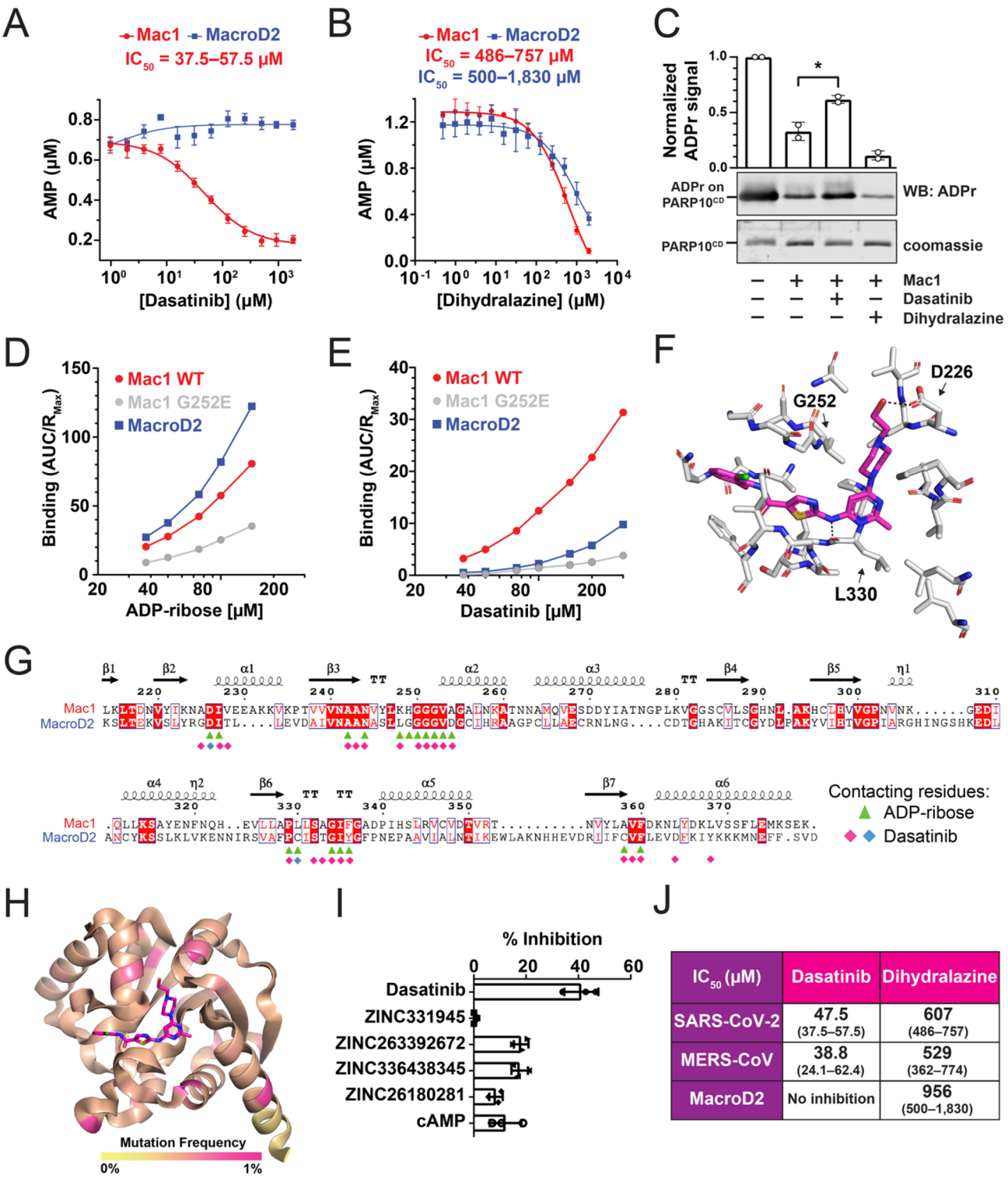

IC_{50} (μM)	Dasatinib	Dihydralazine
SARS-CoV-2	47.5 (37.5–57.5)	607 (486–757)
MERS-CoV	38.8 (24.1–62.4)	529 (362–774)
MacroD2	No inhibition	956 (500–1,830)

Figure 3. Dasatinib inhibits SARS-CoV-2 Mac1 but not human MacroD2. (A,B) Dose−response curves for (A) dasatinib and (B) dihydralazine against SARS-CoV-2 Mac1 and human MacroD2. Plotted values are the mean ± SD (n = 4). (C) Gel-based assay demonstrating the inhibition of Mac1 by dasatinib (n = 2). (D,E) SPR analyses of (D) ADP-ribose and (E) dasatinib binding to Mac1 wild-type (WT) and G252E as well as MacroD2. The binding isotherm was quantitated by the area under the curve (AUC) normalized by the maximal response unit (R_{max}) for each concentration tested in a two-fold dilution series. (F) Molecular docking of dasatinib to Mac1. (G) Structure-based sequence alignment of Mac1 and MacroD2 with residues contacting ADP-ribose (green) and dasatinib, where red and blue indicate hydrophobic and hydrogen-bond (e.g., Asp 226 and Leu 330) interactions, respectively. (H) Analyses of 440 212 SARS-CoV-2 genomes revealed that the dasatinib docking site is highly conserved. No residues within 5 Å of the docking site have a high mutation frequency. (I) Comparison of dasatinib with hits from other SARS-CoV-2 Mac1 high-throughput screens using ADPr-Glo and 100 μM compound. (J) Summary of dasatinib and dihydralazine dose−responses against three macrodomains.

https://doi.org/10.1021/acschembio.1c00721
ACS Chem. Biol. XXXX, XXX, XXX−XXX

macrodomains, we performed surface plasmon resonance (SPR) analyses. Both Mac1 and MacroD2 bound strongly to ADP-ribose (Figure 3D and Figure S5), indicating that both macrodomains were properly folded and able to interact with small-molecule ligands in our SPR assays. Consistent with the selective inhibition observed in the ADPr-Glo assay, dasatinib bound approximately three times more to Mac1 than MacroD2 (Figure 3E and Figure S5). Molecular docking analyses revealed that dasatinib binds at the highly conserved ADP-ribose binding site (Figure 3F−H and Figure S6, Supporting Data File 2), which is supported by the lack of ADP-ribose and dasatinib binding by the active site mutant G252E (Figure 3D−F and Figure S5). Notably, 10 of 25 dasatinib-contacting residues in Mac1 are not conserved in MacroD2 (Figure 3G and Figure S7), which may explain the selectivity.

Recent high-throughput efforts have used virtual and binding screens to identify compounds and fragments that bind to SARS-CoV-2 Mac1 (Figure S8A).[25−27] We directly compared dasatinib to the hits identified in these studies and found that dasatinib was a more potent ADP-ribosylhydrolase inhibitor (Figure 3I and Figure S8B) and a stronger Mac1 binder (Figure S8C). Notably, dasatinib was not identified as a hit despite being included in libraries used by Schuller et al. One possibility is that dasatinib produced high fluorescence when mixed with SYPRO Orange, a dye commonly used in differential scanning fluorimetry (Figure S8D), and may therefore be a false negative in prior screens. These findings collectively highlight the novelty and benefits of our functional screening approach as a complement to existing screens that assay binding.

In summary, we have established a new functional assay to identify ADP-ribosylhydrolase inhibitors. Our facile and versatile assay identifies both specific and general ADP-ribosylhydrolase inhibitors. Our pilot screen identified dasatinib, whose selectivity demonstrates that it is possible to discover drugs that specifically inhibit viral macrodomains. Although cytotoxic when used at micromolar concentration,[28] dasatinib has antiviral activities against SARS-CoV and MERS-CoV through an unknown mechanism.[29] We found that dasatinib also inhibits the MERS-CoV Mac1 macrodomain with similar potency (Figure 3J and Figure S8E,F). Therefore, data presented in this study provide strong support for our target and assay strategy, which can be applied to a large-scale high-throughput screen for new and improved viral macrodomain inhibitors. Because the macrodomain fold is highly conserved in all coronaviruses and alphaviruses, this screening tool represents an important step toward developing new broad-spectrum antivirals.

■ ASSOCIATED CONTENT

Supporting Information

The Supporting Information is available free of charge at https://pubs.acs.org/doi/10.1021/acschembio.1c00721.

Materials and Methods; Supplementary Figures S1−S8: Sequence alignment of coronavirus macrodomains, enzymatic and structural comparisons of SARS-CoV-2 Mac1 and MacroD2, optimizing assay parameters for drug screening, evaluation of pilot screen hits, surface plasmon resonance traces, molecular docking of dasatinib with SARS-CoV-2 Mac1, structure-based sequence alignment of MacroD2 with other human macrodomains, and comparison of dasatinib with hits identified in previously published screens (PDF)

Supplementary Data File 1: Pilot screen raw data (XLSX)

Supplementary Data File 2: Conservation of SARS-CoV-2 genomes (XLSX)

■ AUTHOR INFORMATION

Corresponding Authors

Jürgen Bosch − *Center for Global Health and Diseases, Case Western Reserve University, Cleveland, Ohio 44106, United States; InterRayBio, LLC, Cleveland, Ohio 44106, United States;* orcid.org/0000-0002-2624-4105; Email: jbosch@case.edu

Huijun Wei − *Johns Hopkins Drug Discovery, Baltimore, Maryland 21205, United States; Department of Neurology, School of Medicine, Johns Hopkins University, Baltimore, Maryland 21205, United States;* orcid.org/0000-0003-1961-614X; Email: hwei11@jhmi.edu

Anthony K. L. Leung − *Department of Biochemistry and Molecular Biology, Bloomberg School of Public Health, Johns Hopkins University, Baltimore, Maryland 21205, United States; McKusick-Nathans Department of Genetics Medicine, Department of Oncology, and Department of Molecular Biology and Genetics, School of Medicine, Johns Hopkins University, Baltimore, Maryland 21205, United States;* orcid.org/0000-0001-5569-4036; Email: anthony.leung@jhu.edu

Authors

Morgan Dasovich − *Department of Biochemistry and Molecular Biology, Bloomberg School of Public Health, Johns Hopkins University, Baltimore, Maryland 21205, United States; Department of Chemistry, Krieger School of Arts and Sciences, Johns Hopkins University, Baltimore, Maryland 21218, United States*

Junlin Zhuo − *Department of Biochemistry and Molecular Biology, Bloomberg School of Public Health, Johns Hopkins University, Baltimore, Maryland 21205, United States;* orcid.org/0000-0002-5311-6707

Jack A. Goodman − *Department of Biochemistry and Molecular Biology, Bloomberg School of Public Health, Johns Hopkins University, Baltimore, Maryland 21205, United States*

Ajit Thomas − *Johns Hopkins Drug Discovery, Baltimore, Maryland 21205, United States; Department of Neurology, School of Medicine, Johns Hopkins University, Baltimore, Maryland 21205, United States*

Robert Lyle McPherson − *Department of Biochemistry and Molecular Biology, Bloomberg School of Public Health, Johns Hopkins University, Baltimore, Maryland 21205, United States*

Aravinth Kumar Jayabalan − *Department of Biochemistry and Molecular Biology, Bloomberg School of Public Health, Johns Hopkins University, Baltimore, Maryland 21205, United States*

Veronica F. Busa − *Department of Biochemistry and Molecular Biology, Bloomberg School of Public Health, Johns Hopkins University, Baltimore, Maryland 21205, United States; McKusick-Nathans Department of Genetics Medicine and School of Medicine, Johns Hopkins University, Baltimore, Maryland 21205, United States*

https://doi.org/10.1021/acschembio.1c00721
ACS Chem. Biol. XXXX, XXX, XXX−XXX

Shang-Jung Cheng − *Department of Biochemistry and Molecular Biology, Bloomberg School of Public Health, Johns Hopkins University, Baltimore, Maryland 21205, United States*
Brennan A. Murphy − *Johns Hopkins Drug Discovery, Baltimore, Maryland 21205, United States*
Karli R. Redinger − *Center for Global Health and Diseases, Case Western Reserve University, Cleveland, Ohio 44106, United States*
Yousef M. O. Alhammad − *Department of Molecular Biosciences, University of Kansas, Lawrence, Kansas 66045, United States*
Anthony R. Fehr − *Department of Molecular Biosciences, University of Kansas, Lawrence, Kansas 66045, United States*
Takashi Tsukamoto − *Johns Hopkins Drug Discovery, Baltimore, Maryland 21205, United States; Department of Neurology, School of Medicine, Johns Hopkins University, Baltimore, Maryland 21205, United States;* orcid.org/0000-0002-0216-7520
Barbara S. Slusher − *Johns Hopkins Drug Discovery, Baltimore, Maryland 21205, United States; Department of Neurology, School of Medicine, Johns Hopkins University, Baltimore, Maryland 21205, United States;* orcid.org/0000-0001-9814-4157

Complete contact information is available at: https://pubs.acs.org/10.1021/acschembio.1c00721

Author Contributions

[+]M.D., J.Z., J.A.G., and A.T. contributed equally to this work. Study conception: A.K.L.L.; research design: A.K.L.L., M.D., R.L.M., T.T., B.S., H.W., A.R.F.; data collection: M.D., J.Z., J.A.G., A.T., A.K.J., K.R.R., J.B.; reagent generation: M.D., J.Z., J.A.G., R.L.M., S.-J.C., B.A.M., Y.M.O.A.; data analyses: V.F.B., K.R.R., J.B.; analysis and interpretation of results: M.D., J.B., H.W., A.K.L.L.; draft manuscript preparation: M.D. and A.K.L.L. All authors reviewed the results and approved the final version of the manuscript.

Funding

The work is supported by the COVID-19 PreClinical Research Discovery Fund from Johns Hopkins University (A.K.L.L.) and Johns Hopkins Bloomberg School of Public Health Development Fund (A.K.L.L.).

Notes

The authors declare no competing financial interest.

■ ACKNOWLEDGMENTS

We thank D. Griffin, M. Badiee, and R. Abraham for their critiques of the manuscript. We acknowledge the NudF expression construct from S. Gabelli. We thank L. Bambarger for the initial testing of the luminescence-based assay and S. Goueli for advice on the AMP-Glo assay. Figures 1B and 2A were created with Biorender.com.

■ ABBREVIATIONS

ADP, adenosine diphosphate
SARS, severe acute respiratory syndrome
MERS, Middle East respiratory syndrome
CoV, coronavirus
HIV, human immunodeficiency virus.

■ REFERENCES

(1) Coronaviridae Study Group of the International Committee on Taxonomy of Viruses. The Species Severe Acute Respiratory Syndrome-Related Coronavirus: Classifying 2019-NCoV and Naming It SARS-CoV-2. *Nat. Microbiol.* **2020**, *5* (4), 536−544.
(2) Shyr, Z. A.; Gorshkov, K.; Chen, C. Z.; Zheng, W. Drug Discovery Strategies for SARS-CoV-2. *J. Pharmacol. Exp. Ther.* **2020**, *375* (1), 127−138.
(3) Rack, J. G. M.; Perina, D.; Ahel, I. Macrodomains: Structure, Function, Evolution, and Catalytic Activities. *Annu. Rev. Biochem.* **2016**, *85*, 431−454.
(4) Fehr, A. R.; Jankevicius, G.; Ahel, I.; Perlman, S. Viral Macrodomains: Unique Mediators of Viral Replication and Pathogenesis. *Trends Microbiol.* **2018**, *26* (7), 598−610.
(5) Leung, A. K. L.; McPherson, R. L.; Griffin, D. E. Macrodomain ADP-Ribosylhydrolase and the Pathogenesis of Infectious Diseases. *PLoS Pathog.* **2018**, *14* (3), No. e1006864.
(6) Haikarainen, T.; Lehtiö, L. Proximal ADP-Ribose Hydrolysis in Trypanosomatids Is Catalyzed by a Macrodomain. *Sci. Rep.* **2016**, *6* (1), 24213.
(7) Cho, C.-C.; Lin, M.-H.; Chuang, C.-Y.; Hsu, C.-H. Macro Domain from Middle East Respiratory Syndrome Coronavirus (MERS-CoV) Is an Efficient ADP-Ribose Binding Module: Crystal Structure and Biochemical Studies. *J. Biol. Chem.* **2016**, *291* (10), 4894−4902.
(8) Rosenthal, F.; Feijs, K. L. H.; Frugier, E.; Bonalli, M.; Forst, A. H.; Imhof, R.; Winkler, H. C.; Fischer, D.; Caflisch, A.; Hassa, P. O. Macrodomain-Containing Proteins Are New Mono-ADP-Ribosylhydrolases. *Nat. Struct. Mol. Biol.* **2013**, *20*, 502.
(9) Jankevicius, G.; Hassler, M.; Golia, B.; Rybin, V.; Zacharias, M.; Timinszky, G.; Ladurner, A. G. A Family of Macrodomain Proteins Reverses Cellular Mono-ADP-Ribosylation. *Nat. Struct. Mol. Biol.* **2013**, *20*, 508.
(10) Li, C.; Debing, Y.; Jankevicius, G.; Neyts, J.; Ahel, I.; Coutard, B.; Canard, B. Viral Macro Domains Reverse Protein ADP-Ribosylation. *J. Virol.* **2016**, *90* (19), 8478−8486.
(11) McPherson, R. L.; Abraham, R.; Sreekumar, E.; Ong, S.-E.; Cheng, S.-J.; Baxter, V. K.; Kistemaker, H. A. V.; Filippov, D. V.; Griffin, D. E.; Leung, A. K. L. ADP-Ribosylhydrolase Activity of Chikungunya Virus Macrodomain Is Critical for Virus Replication and Virulence. *Proc. Natl. Acad. Sci. U. S. A.* **2017**, *114* (7), 1666−1671.
(12) Eckei, L.; Krieg, S.; Bütepage, M.; Lehmann, A.; Gross, A.; Lippok, B.; Grimm, A. R.; Kümmerer, B. M.; Rossetti, G.; Lüscher, B.; et al. The Conserved Macrodomains of the Non-Structural Proteins of Chikungunya Virus and Other Pathogenic Positive Strand RNA Viruses Function as Mono-ADP-Ribosylhydrolases. *Sci. Rep.* **2017**, *7*, 41746.
(13) Fehr, A. R.; Channappanavar, R.; Jankevicius, G.; Fett, C.; Zhao, J.; Athmer, J.; Meyerholz, D. K.; Ahel, I.; Perlman, S. The Conserved Coronavirus Macrodomain Promotes Virulence and Suppresses the Innate Immune Response during Severe Acute Respiratory Syndrome Coronavirus Infection. *mBio* **2016**, *7* (6), e01721-16.
(14) Frick, D. N.; Virdi, R. S.; Vuksanovic, N.; Dahal, N.; Silvaggi, N. R. Molecular Basis for ADP-Ribose Binding to the Mac1 Domain of SARS-CoV-2 Nsp3. *Biochemistry* **2020**, *59*, 2608−2615.
(15) Rack, J. G. M.; Zorzini, V.; Zhu, Z.; Schuller, M.; Ahel, D.; Ahel, I. Viral Macrodomains: A Structural and Evolutionary Assessment of the Pharmacological Potential. *Open Biol.* **2020**, *10* (11), 200237.
(16) Alhammad, Y. M. O.; Kashipathy, M. M.; Roy, A.; Gagné, J.-P.; McDonald, P.; Gao, P.; Nonfoux, L.; Battaile, K. P.; Johnson, D. K.; Holmstrom, E. D.; et al. The SARS-CoV-2 Conserved Macrodomain Is a Mono-ADP-Ribosylhydrolase. *J. Virol.* **2021**, e01969-20.
(17) Lin, M.-H.; Chang, S.-C.; Chiu, Y.-C.; Jiang, B.-C.; Wu, T.-H.; Hsu, C.-H. Structural, Biophysical, and Biochemical Elucidation of the SARS-CoV-2 Nonstructural Protein 3 Macro Domain. *ACS Infect. Dis.* **2020**, *6* (11), 2970−2978.

(18) Abraham, R.; Hauer, D.; McPherson, R. L.; Utt, A.; Kirby, I. T.; Cohen, M. S.; Merits, A.; Leung, A. K. L.; Griffin, D. E. ADP-Ribosyl−Binding and Hydrolase Activities of the Alphavirus NsP3Macrodomain Are Critical for Initiation of Virus Replication. *Proc. Natl. Acad. Sci. U. S. A.* **2018**, *115* (44), E10457−E10466.
(19) Abraham, R.; McPherson, R. L.; Dasovich, M.; Badiee, M.; Leung, A. K. L.; Griffin, D. E. Both ADP-Ribosyl-Binding and Hydrolase Activities of the Alphavirus NsP3Macrodomain Affect Neurovirulence in Mice. *mBio* **2020**, *11* (1), e03253-19.
(20) Eriksson, K. K.; Cervantes-Barragán, L.; Ludewig, B.; Thiel, V. Mouse Hepatitis Virus Liver Pathology Is Dependent on ADP-Ribose-1″-Phosphatase, a Viral Function Conserved in the Alpha-like Supergroup. *J. Virol.* **2008**, *82* (24), 12325−12334.
(21) Voth, L. S.; O'Connor, J. J.; Kerr, C. M.; Doerger, E.; Schwarting, N.; Sperstad, P.; Johnson, D. K.; Fehr, A. R. An MHV Macrodomain Mutant Predicted to Lack ADP-Ribose Binding Activity Is Severely Attenuated, Indicating Multiple Roles for the Macrodomain in Coronavirus Replication. *J. Virol.* **2021**, *95*, e00766-21.
(22) Jayabalan, A. K.; Adivarahan, S.; Koppula, A.; Abraham, R.; Batish, M.; Zenklusen, D.; Griffin, D. E.; Leung, A. K. L. Stress Granule Formation, Disassembly, and Composition Are Regulated by Alphavirus ADP-Ribosylhydrolase Activity. *Proc. Natl. Acad. Sci. U. S. A.* **2021**, *118* (6), e2021719118.
(23) Daniels, C. M.; Thirawatananond, P.; Ong, S.-E.; Gabelli, S. B.; Leung, A. K. L. Nudix Hydrolases Degrade Protein-Conjugated ADP-Ribose. *Sci. Rep.* **2016**, *5*, 18271.
(24) Baell, J. B.; Holloway, G. A. New Substructure Filters for Removal of Pan Assay Interference Compounds (PAINS) from Screening Libraries and for Their Exclusion in Bioassays. *J. Med. Chem.* **2010**, *53* (7), 2719−2740.
(25) Schuller, M.; Correy, G. J.; Gahbauer, S.; Fearon, D.; Wu, T.; Díaz, R. E.; Young, I. D.; Carvalho Martins, L.; Smith, D. H.; Schulze-Gahmen, U.; et al. Fragment Binding to the Nsp3Macrodomain of SARS-CoV-2 Identified through Crystallographic Screening and Computational Docking. *Science Advances* **2021**, *7* (16), No. eabf8711.
(26) Virdi, R. S.; Bavisotto, R. V.; Hopper, N. C.; Vuksanovic, N.; Melkonian, T. R.; Silvaggi, N. R.; Frick, D. N. Discovery of Drug-Like Ligands for the Mac1 Domain of SARS-CoV-2 Nsp3. *SLAS Discov* **2020**, *25* (10), 1162−1170.
(27) Bajusz, D.; Wade, W. S.; Satała, G.; Bojarski, A. J.; Ilaš, J.; Ebner, J.; Grebien, F.; Papp, H.; Jakab, F.; Douangamath.; et al. Exploring Protein Hotspots by Optimized Fragment Pharmacophores. *Nat. Commun.* **2021**, *12* (1), 3201.
(28) Hochhaus, A.; Kantarjian, H. M.; Baccarani, M.; Lipton, J. H.; Apperley, J. F.; Druker, B. J.; Facon, T.; Goldberg, S. L.; Cervantes, F.; Niederwieser, D.; et al. Dasatinib Induces Notable Hematologic and Cytogenetic Responses in Chronic-Phase Chronic Myeloid Leukemia after Failure of Imatinib Therapy. *Blood* **2007**, *109* (6), 2303−2309.
(29) Dyall, J.; Coleman, C. M.; Hart, B. J.; Venkataraman, T.; Holbrook, M. R.; Kindrachuk, J.; Johnson, R. F.; Olinger, G. G., Jr; Jahrling, P. B.; Laidlaw, M.; et al. Repurposing of Clinically Developed Drugs for Treatment of Middle East Respiratory Syndrome Coronavirus Infection. *Antimicrob. Agents Chemother.* **2014**, *58* (8), 4885−4893.

https://doi.org/10.1021/acschembio.1c00721
ACS Chem. Biol. XXXX, XXX, XXX−XXX